Applied Microbiology and Biotechnology (2018) 102:4049–4061
https://doi.org/10.1007/s00253-018-8875-y

BIOTECHNOLOGICALLY RELEVANT ENZYMES AND PROTEINS

Four second-sphere residues of *Thermus thermophilus* SG0.5JP17-16 laccase tune the catalysis by hydrogen-bonding networks

Huiping Liu [1,2] · Yanyun Zhu [1,2] · Xiaorong Yang [1,2] · Ying Lin [1,2]

Received: 19 November 2017 / Revised: 6 February 2018 / Accepted: 13 February 2018 / Published online: 7 March 2018

Abstract

The multicopper oxidases catalyze 1-electron oxidation of four substrate molecules and concomitantly 4-electron reduction of dioxygen to water. The substrate loses the electrons at the type 1 copper (T1 Cu) site of the enzyme, while the dioxygen is reduced to water at the trinuclear copper center. A highly conserved Glu residue, which is at the dioxygen-entering channel, shuttles the proton to break the O-O bond of dioxygen. At the water-leaving channel, an Asp residue was found to be important in the protonation mechanism. In this study, laccase from *Thermus thermophilus* SG0.5JP17-16 (lacTT) was investigated to address how four second-sphere residues E356, E456, D106, and D423 affect the activity of the enzyme. Kinetic data indicate that catalytic activities of the enzyme are altered by site-directed mutagenesis on four second-sphere residues. The structural model of lacTT was generated by homology modeling. Structural and spectral data indicate that the E356 residue is situated at the substrate-binding site, responsible for the binding of the substrate and the geometry of the T1 Cu site by hydrogen-bonding networks; the E456 residue, located at the dioxygen-entering channel, plays a critical role in stabilizing the structure of all active copper centers and shuttling the proton to the trinuclear copper cluster (TNC) for the reductive reaction of dioxygen; the D106 and D423 residues are at the water-leaving channel, and they are important for the essential geometry of the TNC and the release of the water molecules. Altogether, this study contributes to the further understanding of the basic mechanism involving the oxidation of the substrate, electron transfer, and the reduction of dioxygen in lacTT.

Keywords Bacterial laccase · Enzyme mechanism · Enzyme kinetics · Homology modeling · Hydrogen-bonding network

Introduction

The multicopper oxidases (MCOs) constitute a family of enzymes known to oxidize a variety of organic and/or inorganic substrates (Solomon et al. 2014; Santhanam et al. 2011; Pezzella et al. 2015; Dwivedi et al. 2011). They are widely distributed in fungi, bacteria, plants, and insects, involved in lignin formation in plant, pigment formation in fungi, copper homeostasis in bacteria, and iron metabolism in yeast (Nakamura and Go 2005; Giardina et al. 2010).

Laccases are one of the simplest members in the MCO family. Structurally, they exhibit a similar overall fold composed of three cupredoxin-like domains and a catalytic motif containing four copper atoms. Four copper atoms were classified into three types according to their spectroscopic features (Malmstrom 1982; Silva et al. 2012; Jones and Solomon 2015). The type 1 copper (T1 Cu) was characterized by an intense absorption band of the S(Cys) → Cu(II) charge transfer (CT) at around 600 nm, and a small parallel hyperfine coupling in electron paramagnetic resonance (EPR) (Jones and Solomon 2015). The type 2 copper (T2 Cu) exhibited no distinctive absorption features but a large parallel hyperfine coupling in EPR (Jones and Solomon 2015). Two type 3 coppers (T3 Cu) were anti-ferromagnetically coupled through a

Electronic supplementary material The online version of this article (https://doi.org/10.1007/s00253-018-8875-y) contains supplementary material, which is available to authorized users.

✉ Xiaorong Yang
birxyang@scut.edu.cn

✉ Ying Lin
feylin@scut.edu.cn

[1] Guangdong Provincial Key Laboratory of Fermentation and Enzyme Engineering, School of Biology and Biological Engineering, South China University of Technology, Guangzhou 510006, People's Republic of China

[2] Guangdong Research Center of Industrial Enzyme and Green Manufacturing Technology, School of Biology and Biological Engineering, South China University of Technology, 334 Building 6, University Park, Guangzhou 510006, People's Republic of China

bridging hydroxide and consequently EPR is silent, but they exhibited a CT transition at around 330 nm (Chen et al. 2010). The T2 Cu and T3 Cu formed the trinuclear copper cluster (TNC).

The electron transfer (ET) in laccases includes intermolecular ET from the substrate to the T1 Cu ion, and intramolecular ET from the T1 Cu ion to the TNC via a conserved His-Cys-His triad (Wherland et al. 2014; Enguita et al. 2004). The oxidation of the substrate occurs at the T1 Cu site (Enguita et al. 2004). It is suggested that the solvent-exposed His residue, a first-sphere ligand of the T1 Cu atom, was at the substrate-binding site common in laccase, and it might be responsible for the electron transfer from the substrate to the T1 Cu ion (Matera et al. 2008; Polyakov et al. 2009; Kallio et al. 2009). The electrons were transferred at ~ 13 Å within the protein from the T1 Cu site to the TNC. At the TNC, the O_2 molecule was bound, activated, and reduced to H_2O (Jones and Solomon 2015; Wherland et al. 2014). The four-electron reduction process of O_2 to two H_2O molecules requires four protons and four electrons. Based on the sequence alignment and known crystal structures, two highly conserved carboxylate residues located close to the TNC were found to be involved in O_2 reduction (Jones and Solomon 2015; Hugo et al. 2015). One Glu or Asp residue is situated at the dioxygen-entering channel. One Asp residue is situated at the water-leaving channel (Chen et al. 2010). Two acidic residues may facilitate the binding of O_2, supply of protons, and cleavage of the O-O bond as indicated by studies performed on Fet3p-metallo oxidase from *Saccharomyces cerevisiae*, *Tth*-MCO from *Thermus thermophilus* HB27, CotA-laccase from *Bacillus subtilis*, and CueO-laccase from *Escherichia coli* (Santhanam et al. 2011; Hugo et al. 2015; Quintanar et al. 2005; Augustine et al. 2007; Silva et al. 2012; Chen et al. 2010; Bento et al. 2010; Kataoka et al. 2009; Ueki et al. 2006).

Our previous work demonstrated that *T. thermophilus* SG0.5JP17-16 laccase (lacTT) is thermoactive and chloride-tolerant, and it can degrade some synthetic dyes (Liu et al. 2015). Thus, the lacTT is a good candidate for the decolorization and detoxification of textile wastewaters. In this study, we built the 3D–structural model of lacTT and, in addition, analyzed the roles of two carboxylate residues E456 and D106 which are equivalent to those found in other MCOs (Hugo et al. 2015; Quintanar et al. 2005; Augustine et al. 2007; Kataoka et al. 2009; Ueki et al. 2006). For the first time, we identified another two key residues, E356 and D423 in lacTT, and explored their roles. The E356 residue may be important for the binding of the substrate and geometry of the T1 Cu site. The D423 residue may have similar function to that of the D106 residue. Furthermore, we developed the catalytic mechanism of laccase, which can provide a new strategy to modify the laccase for the industrial applications, for example, the treatment of synthetic dyestuff.

Materials and methods

Structural modeling and molecular docking

The laccase from *Thermus thermophilus* HB27 has 75% primary amino acid sequence identity to lacTT. The crystal structure of *Thermus thermophilus* HB27 laccase (lacHB27) was taken from the Protein Data Bank (PDB ID: 2XU9A) and used as the template to build the 3D model of lacTT. Modeling analysis was done by Discovery Studio Client 3.5 (DS 3.5, Accelrys, Inc., San Diego, CA, USA). The rationality of the 3D model for lacTT was examined via Ramachandran plot and Profile-3D scoring. The protein design procedure was used to build the mutants. Molecular docking was performed using an automated Dock Ligands subprogram of DS 3.5 to fit the substrate guaiacol into the model structure of lacTT; hydrogen bonds and bond lengths were analyzed.

Mutagenesis, expression, and purification

The lacTT gene was optimized for *E. coli* expression using Optimum Gene technology and synthesized by GenScript Biotech Co. (Nanjing, China). The accession number of the codon-optimized lacTT gene was BankIt2067778 (Seq1MG601742) in GenBank. Amplification of the laccase gene was performed by PCR using the primers TT-F/TT-R (Table S1) and the synthesized laccase gene as the template. Single amino acid substitutions were created using overlap extension PCR with the primers shown in Table S1. The wild-type and mutated genes (E356A, D106L, D106R, D106E, E456L, E456R, E456D, and D423A) were cloned into the *Nco* I and *Hin*d III sites of plasmid pET-30a(+) (Novagen, Madison, WI) and expressed in *E. coli* BL21(DE3) (Novagen, Madison, WI).

E. coli BL21(DE3) containing recombinant plasmids were grown in Luria-Bertani (LB) medium supplemented with kanamycin (50 μg/mL) at 37 °C and 200 rpm. When the OD_{600} of the culture reached 0.6–1.0, 0.1 mM IPTG was added to induce protein expression, and the cells were grown for another 12–18 h, with shaking at 30 °C and 200 rpm. The cells were harvested by centrifugation, then resuspended in Buffer A (20 mM Tris-HCl, 500 mM NaCl, pH 7.5) containing 0.2 mM $CuSO_4$, and sonicated on ice. The crude cell extracts were centrifuged at 8000×*g* for 30 min. The supernatant was collected, and the soluble wild-type (WT), E356A, D106L, D106R, D106E, E456L, E456R, E456D, and D423A lacTT proteins were purified by immobilized metal affinity chromatography (IMAC). The purification was performed with HisTrap™ FF crude column (GE Healthcare) using AKTA purifier FPLC system (GE Healthcare). The purity of the purified protein was checked by sodium dodecyl sulfate polyacrylamide gel electrophoresis (SDS-PAGE). Protein

concentration was estimated using Bradford assay with bovine serum albumin (BSA) (Sigma-Aldrich) as the standard.

Enzymatic activity assay

A standard enzyme activity assay was performed in a 1.0-mL reaction mixture containing 50 mM sodium phosphate buffer (pH 6.0), 10 μM $CuSO_4$ and 2.0 mM guaiacol (ε_{465} = 12,000 M^{-1} cm^{-1}). The reaction started with the addition of enzymes at 90 °C. After incubation at 90 °C for 5 min, the mixture was immediately cooled in ice bath for 1 min to stop the reaction, and the absorbance was measured at 465 nm. One unit of enzyme was defined as the amount of enzyme that oxidizes 1 μmol guaiacol per minute.

Biochemical characterization

The enzymatic activities were recorded at 90 °C in Britton–Robinson buffer as the function of the pH values varying from 4.5–8.0, using guaiacol as substrate. The optimal pH values for lacTT and its mutants were determined (Fig. S1); no difference in the pH behavior was observed between mutants D106R, D106E, E456R, and wild-type lacTT, and the optimal pH value was 6.0. However, the optimal pH values of D106L, E356A, and D423A mutants moved slightly towards acidic value by 0.5 or 1 units. The optimal pH values of E456L and E456D mutants increased by 1.5 and 2 units, respectively. Figure S2 shows the enzymatic activity as a function of the temperature in the range of 60–95 °C. Optimal reaction temperatures of the wild-type enzyme and mutants were determined for 50 mM sodium phosphate buffer at pH 6. Except for the D106R mutant, which exhibits an optimal temperature of 80 °C, wild-type lacTT and other mutants display similar optimal temperature of 90 °C (Fig. S2). The thermostability of the enzymes was examined for 80 °C during 4 h. D106E and E456R mutants exhibit similar thermal stability to that of wild-type lacTT; the thermostability of the other mutants is reduced (Fig. S3). All assays were repeated for three times.

Kinetic studies

Kinetic assay was performed for wild-type lacTT and mutants in 50 mM sodium phosphate buffer (pH 6.0), supplemented with 10 μM $CuSO_4$ and 0.125–4.0 mM guaiacol in air saturated conditions as described previously (Durao et al. 2006). The reaction started with the addition of enzymes at 90 °C. Kinetic parameters were obtained by fitting the data to the Lineweaver–Burk plot. All assays were repeated for three times.

UV-visible spectroscopy

UV-visible absorption spectra (300–800 nm) of the purified proteins were recorded by using a Hitachi U-3010 spectrophotometer at room temperature in 10 mM sodium phosphate buffer (pH 6.0). The concentration of the protein was 3 mg/ml.

CD spectroscopy

Far-UV circular dichroism (CD) spectra (190 to 260 nm) were recorded by using an Applied Photophysics Chirascan spectrometer at room temperature in 10 mM sodium phosphate (pH 6.0). The bandwidth in a 1-mm cell was 1 nm. The protein concentration was 0.3 mg/ml. Data were averaged, and the baselines were subtracted.

Results

Structural model of lacTT

So far, the structure of lacTT has not been available; therefore, we used homology modeling to build its three-dimensional structure. In order to select an appropriate template, we employed BLASTp to search PDB. It was found that lacHB27 (PDB entry: 2XU9A) has 75% sequence identical to that of lacTT, and the crystallographic structure of lacHB27 was resolved (Hugo et al. 2015). Based on homology modeling and energy minimization, the structural model of lacTT was generated, and it is presented in Fig. 1a. The quality of the model was evaluated by Ramachandran plot and Profile-3D. In Ramachandran plot, 93.4% of the amino acid residues were located in the optimum region, 3.4% were in the allowed region, and only 2.7% in the disallowed region (Fig. 1b). In Profile-3D graph, the compatibility score of the amino acid residues was 98.9% (Fig. 1c). Thus, the generated model can represent the structure of lacTT, and it will be employed in the following analyses.

Like other MCO structures (Hugo et al. 2015; Piontek et al. 2002; Enguita et al. 2003; Bello et al. 2012), the structural model of lacTT contains three cupredoxin-like domains and four copper atoms classified into two active sites, a mononuclear T1 Cu center situated in domain 3 and a TNC located at the interface between domains 1 and 3 (Fig. 1a). The active Cu sites of lacTT share primary coordination sphere characteristics of other bacterial MCOs. The T1 Cu atom is beset in a tetrahedral geometry formed by His397, His455, Cys450, and Met460 residues (Fig. 1d), where the substrate was oxidized. In UV-visible spectrum (Fig. 2a), a strong absorption band appeared at around 608 nm due to the charge transfer transition between S_{cys450} and T1 Cu^{2+} (Solomon 2006). There is a methionine-rich motif on the top of the substrate-binding

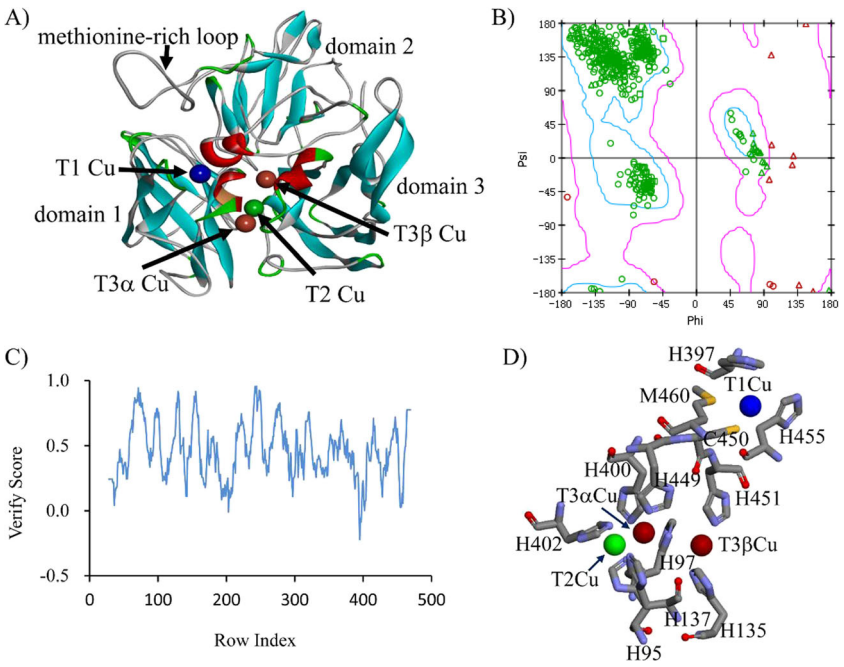

Fig. 1 Structural model of lacTT. **a** The modeled three-dimensional structure of lacTT comprised of three domains, showing α-helices in red, β-sheets in cyan, β-turns in green, loops in gray, T1 Cu in blue and trinuclear copper cluster (TNC): T2 Cu in green, and two T3 Cu in dark red. **b** Ramachandran plot of the simulated lacTT structure, showing the residues in the optimum region (blue), the allowed region (magenta), and the disallowed region (red triangle). **c** Profile-3D of the lacTT structure, indicating the compatibility score of the majority of the residues was greater than zero. **d** The geometry of the copper active sites: the copper ions (spheres) and their ligands

pocket. The TNC is comprised of a T2 Cu and two T3 Cu atoms (denoted as T3α Cu and T3β Cu). The T3α Cu coordinated by His137, His402, and His449 residues is ~ 5 Å away from the T3β Cu having His97, His135, and His451 ligands (Fig. 1d). At about 330 nm of the UV-visible spectrum, a broad shoulder absorption band was recorded, and it is due to the charge transfer transition between the T3 Cu ions and a hydroxyl bridged between

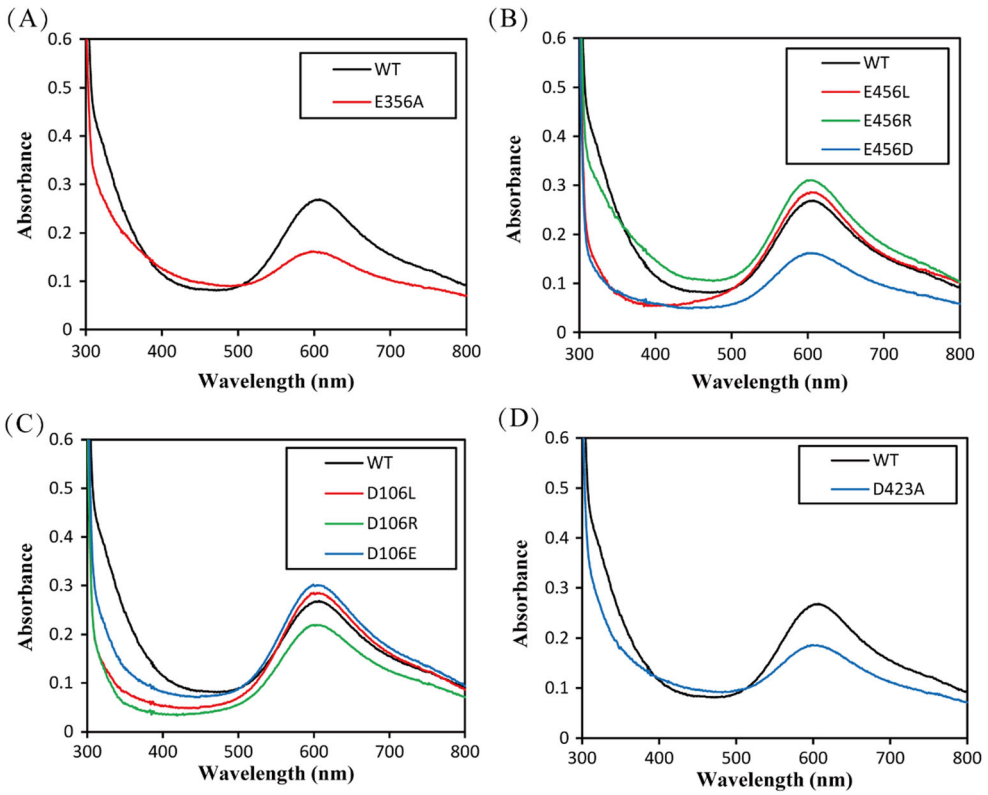

Fig. 2 UV-visible absorption spectra of the lacTT proteins were measured at room temperature in 10 mM sodium phosphate buffer, pH 6.0. The protein concentration was 3 mg/ml. **a** WT (black) and E356A (red). **b** WT (black) and E456D (blue), and E456R (green) and D456L (red) mutants. **c** WT (black) and D106E (blue), and D106R (green) and D106L (red) mutants. **d** WT (black) and D423A (blue)

two T3 Cu ions (Cole et al. 1990). The T2 Cu atom is braced by His95 and His400 residues; no absorption band was observed for the T2 Cu atom.

The effect of a second-sphere Glu residue at the T1 Cu site on the oxidation of the substrate

It is well known that in MCOs, the substrate is oxidized at the T1 Cu site, and the intermolecular ET from the substrate to the T1 Cu ion is controlled most likely by the ligands surround the T1 Cu ion (Kataoka et al. 2007; Marcus and Sutin 1985). The geometry formed by the primary coordination ligands was tuned by the second-sphere residues via H-bonding networks (Span et al. 2017). In lacTT, the second-sphere residues comprise E356, which is located at the T1 Cu site and is H-bonded to the His397 ligand of the T1 Cu atom, Glu456, D106, and D423. The later three residues are positioned close to the TNC (Fig. 3).

In order to further understand the role of the E356 residue, we mutated Glu356 to Ala356. CD spectra of the WT laccase and the E356A mutant are similar, as shown in Fig. 4a, suggesting that the global structure of the enzyme is not affected by site-directed substitution of the E356 residue. The distance between copper ions in the E356A mutant is identical to that in the wild-type enzyme as reported in Table S2. Thus, the replacement of the E356 residue by alanine does not affect the relative position of the active Cu sites. We characterized the biochemical properties of the E356A mutant. The optimal pH value of the E356A mutant is the same as that of WT enzyme, which is approximately 6.0 (Fig. S1A). However, the kinetic study suggests that the catalytic efficiency (K_{cat}/K_m) of the E356A enzyme decreased ~13-fold as compared to that of WT laccase, as it can be observed in Table 1. The comparison of UV-visible spectra for WT laccase and the E356A variant reveals that the absorption intensity is similar at 330 nm, but the absorption intensity at 608 nm for the E356A mutant is 60% of the wild-type enzyme (Fig. 2a and Table S3), reflecting the lower Cu loading at the T1 Cu site in the mutant. Thus, the efficiency of the E356A mutant should be adjusted to eightfold lower than that of the wild-type laccase. From the structural model of lacTT, the side chain $O^{\varepsilon 1}$ atom of the E356 residue is 4.7 Å away from the side chain N^{δ} atom of His397. They can form the H-bond interaction, while the E356 residue is negative charged at the optimal pH 6.0, the carboxyl group of the E356 residue may H-bond to the side chain N^{ε} atom of His397 (Fig. 5a). These interactions are required to retain the geometry of the T1 Cu site and to enhance the nucleophilicity of the His ligand. The substitution of the E356 residue by an apolar alanine eliminated these interactions. The side chain of the A356 residue pointed to the opposite direction of the H397 ligand (Fig. 5b). The kinetic assay showed that the K_{cat} value of the E356A mutant decreased ~4-fold, while the K_m value increased ~4-fold relative to that of WT enzyme (Table 1). We compared the substrate-binding pockets in WT enzyme (Fig. 6a) and the E356A mutant (Fig. 6b). The pocket in the E356A mutant became deeper, suggesting that the E356 residue is related to the binding of the substrate, for example, probably responsible for holding the substrate at the correct position to form the optimal interactions between the substrate and the catalytic residues from the enzyme. Therefore, we inferred that the E356 residues, serving as a secondary coordination sphere residue, affected the catalysis of the enzyme mainly by orientating the histidine ligands of the T1 Cu atom and/or the binding of the substrate. We tried to further clarify

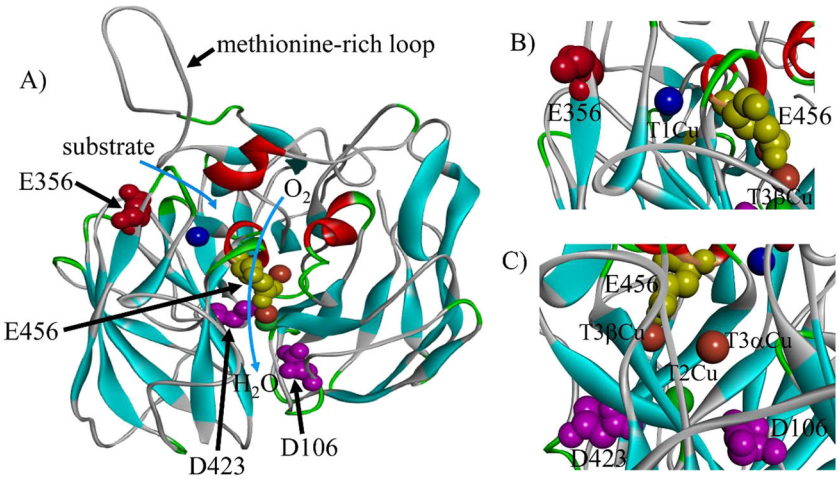

Fig. 3 **a** Four second-sphere residues distributed in the lacTT. The color scheme is same as that in Fig. 1. The E356 residue (red) is located at the T1 Cu site and in the region of the substrate binding. At the top of the T1 Cu site, there is a methionine-rich loop, which may be a switch of controlling the substrate entering. The E456 residue (yellow) is between the T1 Cu site and the TNC, at the O_2-entering channel. The D423 residue (magenta) is at the T2-T3β Cu atom side of the TNC. The residue D106 (magenta) is set to the T2-T3α Cu atom side of the TNC, at the exit of the reduced water. **b** The zoom-in of the T1 Cu center highlighting the locations of the residues E356 and E456. **c** The zoom-in of the TNC center highlighting the locations of the residues E456, D423, and D106

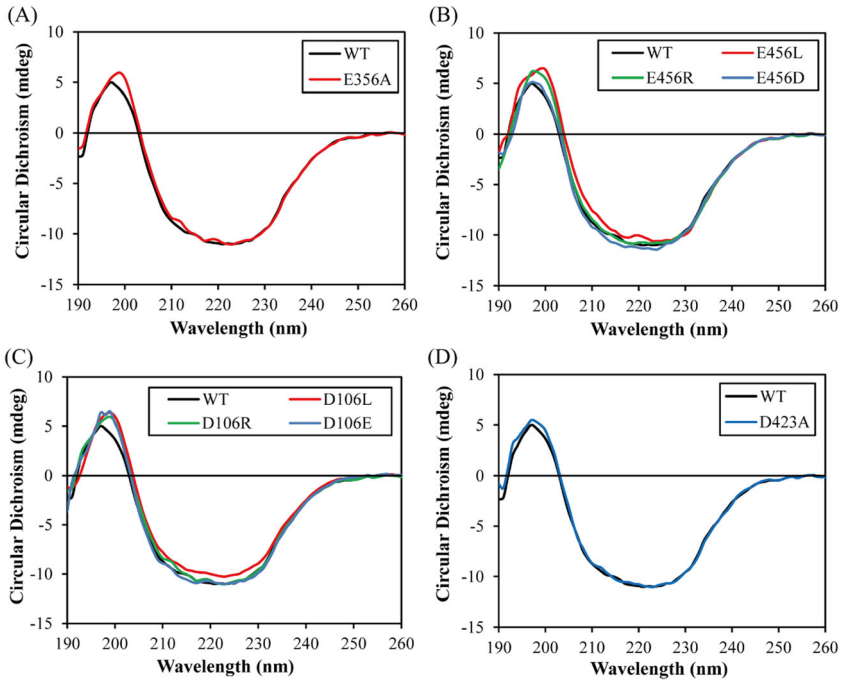

Fig. 4 CD spectra of the lacTT proteins were measured at room temperature in 10 mM sodium phosphate buffer, pH 6.0. The protein concentration was 3 mg/ml. **a** WT (black) and E356A (red). **b** WT (black) and E456D (blue), E456R (green), and D456L (red) mutants. **c** WT (black) and D106E (blue), and D106R (green) and D106L (red) mutants. **d** WT (black) and D423A (blue)

the details of the interactions between the substrate and the enzyme via the docking study. Unfortunately, the substrate could not be docked into the substrate-binding pocket, as shown in Fig. S4, most probably due to the closed conformation of the methionine-rich loop blocking the entering of the substrates.

The electric transfer from T1 Cu to TNC coordinated by a Glu residue at the TNC

The electron was abstracted at the T1 Cu site, then, rapidly transferred to the TNC via the Cys-His pathway. At the TNC, the dioxygen obtained the electrons and was reduced to the water (Jones and Solomon 2015). The bioinformatics analysis based on the sequence identity and structure revealed that the residues Glu456, D106, and D423 in lacTT are highly conserved (Figs. 3 and S5), and would control the intramolecular electron transfer from T1 Cu to the TNC, the reduction of the dioxygen, and/or the release of the water.

The G456 residue was located between the T1 Cu site and T3α Cu atom. Its carboxyl side chain points towards the O_2-entering channel, within the H-bond distance with the histidine ligands of the T3α Cu atom. The distances from the side chain O^{ε} atoms of the Glu456 residue to the $N^{\delta 1}$ atom of His449 and the $N^{\delta 1}$ atom of His137 are 4.79 and 3.46 Å, respectively (Fig. 7a); consequently, this residue is important for the geometry of the TNC. The E456 residue in lacTT is equivalent to Glu451 in lacHB27, Glu498 in the CotA-laccase, Glu506 in the CueO-laccase, and Glu487 in Fet3p-metallo oxidase (Hugo et al. 2015; Chen et al. 2010; Bento et al. 2010; Quintanar et al. 2005; Augustine et al. 2007; Kataoka et al. 2009; Ueki et al. 2006). Previous studies show that the acidic residue at this position is involved in the proton transfer procedure during the dioxygen reduction to the water (Hugo et al. 2015; Chen et al. 2010; Bento et al. 2010; Quintanar et al. 2005; Augustine et al. 2007; Kataoka et al. 2009; Ueki et al. 2006). To examine its ability to shuttle the proton, the E456 residue was replaced by the leucine, arginine, and aspartic acid, respectively, by site-directed mutagenesis. The catalytic activities of WT lacTT and its mutants were determined by using the guaiacol as the reducing substrate at their optimum pH value. Compared with the wild-type enzyme, the E456L, E456R, and E456D mutants exhibited lower catalytic efficiencies (k_{cat}/K_m), shown in Table 1. The catalytic efficiency of the E456D mutant decreased eightfold. The below UV-visible spectral data revealed that 61% of population of the T1 Cu site in the E456D mutant were filled with the

Table 1 Apparent steady-state kinetic constants measured at the saturating concentrations of O_2 for guaiacol by the lacTT proteins

LacTT	K_m (μM)	k_{cat} (s^{-1})	k_{cat}/K_m (s^{-1} mM^{-1})
Wild type	384 ± 34	6.1 ± 0.15	16 ± 1.5
E356A	1466 ± 144	1.70 ± 0.16	1.16 ± 0.07
E456L	135 ± 23	0.059 ± 0.007	0.44 ± 0.03
E456R	512 ± 44	0.32 ± 0.02	0.62 ± 0.03
E456D	380 ± 15	0.78 ± 0.01	2.1 ± 0.09
D106L	488 ± 4	2.1 ± 0.02	4.3 ± 0.02
D106R	689 ± 55	2.3 ± 0.1	3.3 ± 0.08
D106E	458 ± 25	2.2 ± 0.07	4.8 ± 0.15
D423A	476 ± 24	3.51 ± 0.22	7.37 ± 0.14

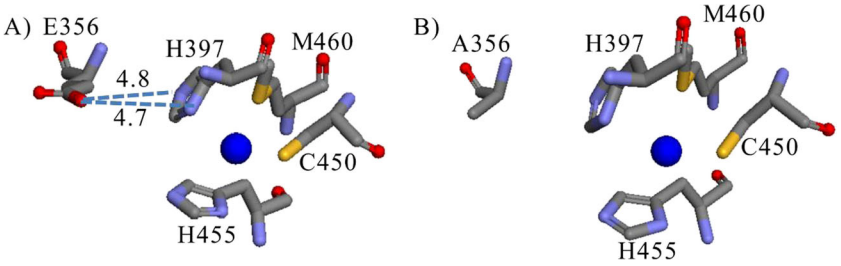

Fig. 5 Hydrogen-bonding networks between T1 Cu ligands and the E356 residue. The T1 Cu atom is braced in a tetrahedral geometry formed by the residues M460, C450, H455, and H397. **a** The E356 residue is within hydrogen-bonding distance with the H397 residue, a ligand of the T1 Cu atom. **b** The A356 residue cannot form the H-bond interaction with the H397 residue

copper atoms (Table S3); the efficiency of the E456D mutant should be adjusted to fivefold lower than that of the wild-type laccase. The aspartic acid had the ability to shuttle the proton, but the transfer efficiency became lower due to the shorter side chain than that of glutamic acid. In E456L and E456R mutants, the apolar leucine and the basic arginine residues at the reaction pH value could not channel the proton for the reduction of the dioxygen, the E456L and E456R mutants showed 30 to 40 times lower efficiency in relation to the wild type.

In the UV-visible spectrum, the wild-type lacTT presented two absorption bands. One maximum absorption band appeared at 608 nm, and the other at 330 nm. The E456D mutant showed two lower intensity peaks; the maximum absorption intensity at 608 nm was 61% of the wild-type enzyme (Fig. 2b and Table S3). After treatment with potassium bichromate, this absorption intensity did not change; ruling out that the reduction of the T1 Cu ion resulted in the decrease of the peak intensity for the E456D mutant. Thus, some of T1 Cu sites in the E456D mutant lack copper. The E456L and E456R mutants show higher peak intensity at 608 nm compared to the wild-type enzyme, reflecting that the occupancy of T1 Cu sites in two mutants is slightly higher. CD spectra of three variants were similar to that of the wild-type laccase, as shown in Fig. 4b. The structure of each mutant can superimpose well that of the wild-type laccase (Fig. S6C). These data clearly indicate that their overall structures are essentially the same. However, the differences are also observed for the copper centers and their surrounds; the distances between three coppers at the TNC in three mutants increase, as shown in Table S2. The E456R mutant was most affected, showing the longest distance between any two coppers. These findings reflect a loose structure at the TNC center in terms of the variants, which might be related to a slower electron transfer rate, consistent with the lower K_{cat} value for variants.

In the wild-type lacTT, the E456 residue is situated next to the T3α Cu atom and its carboxyl side chain points towards the T3α Cu (Fig. 3). The side chain $O^{\varepsilon 2}$ atom of Glu456 was 2.98 Å away from the N^{ε} atom of His449 and 3.74 Å from the N^{ε} atom of His137 (Fig. 7a). In the E456D mutant, aspartic acid residue has a shorter side chain, and the orientation of the side chain is altered, which increases the distances from the side chain O^{δ} atom of Asp456 to His449 and His137 ligands of the T3α Cu atom to 3.92 and 4.43 Å, respectively (Fig. 7b), resulting in the orientation change of the His ligands and/or the decrease of the interactions between the His ligands and the D456 residue. Furthermore, these effects are transferred to His135, His451, and Cys450 via β-sheets, and to His455 via α-helix (ligands of T3β and T1 Cu atoms). It is suggested that, in E456D mutant, the coordination of all Cu centers can be affected. These results are consistent with the intensity alteration of the absorption peaks in the UV-visible spectra and the change of the distances between any two coppers in the mutant described above. The alteration of interacting networks and the ligand orientation of the Cu atoms are also observed in the E456R and E456L mutants. In the E456R mutant, the longer, positively charged side chain of the R456 residue is extended to H-bond distance with the His135 and His451 ligands of the T3β Cu atom (Fig. 7c). In the E456L mutant,

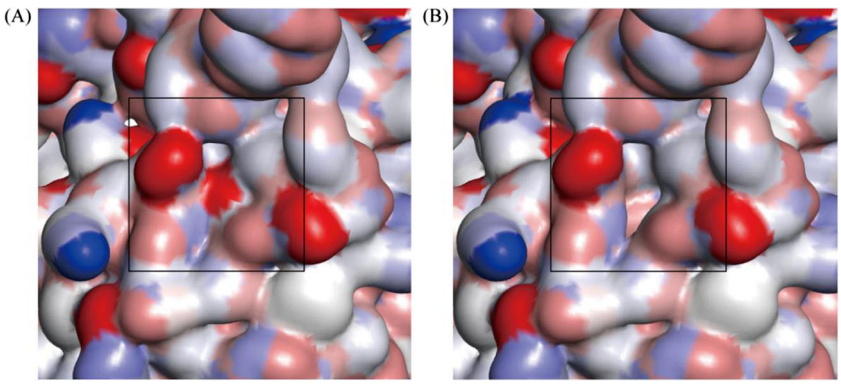

Fig. 6 Surface presentation showed the shape of the substrate-binding pockets for the wild-type lacTT (**a**) and the E356A mutant (**b**). The Glu356 residue in the substrate-binding pocket is in red. The substitution of the E356 residue by alanine resulted in a deeper pocket

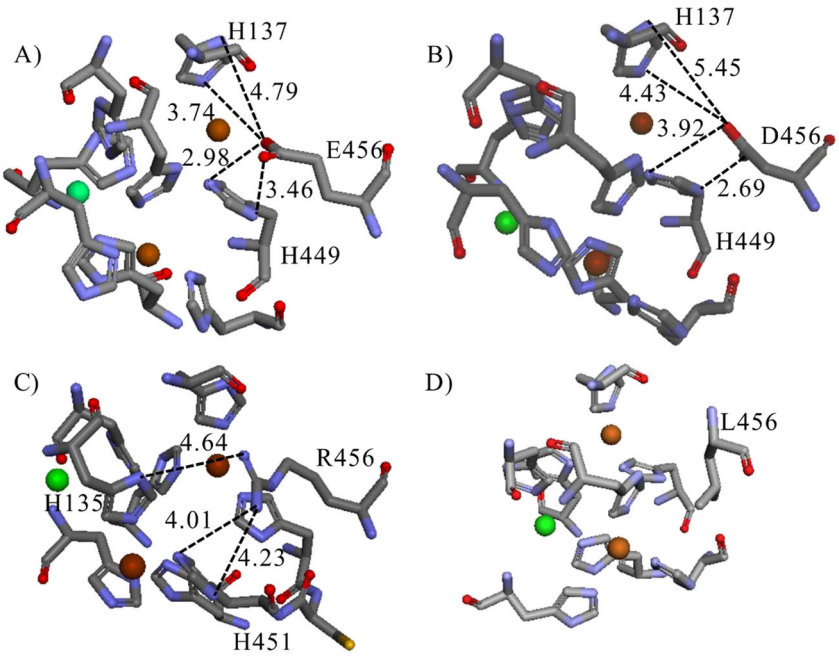

Fig. 7 Hydrogen-bonding networks formed between the amino acid residue at the position of 456 and the histidine ligands of the copper centers. **a** In the wild-type lacTT. **b** In the E456D mutant. **c** In the E456R mutant. **d** In the E456L mutant

these interactions could not be formed, and the orientation of the L456 residue was altered (Fig. 7d), the catalytic behavior of the enzyme was changed. By combining the structural, UV-visible and CD spectral data, it was found out that the secondary coordination sphere residue E456, apart from channeling the proton for the reduction of the O_2 molecule (Chen et al. 2010; Hugo et al. 2015; Kataoka et al. 2009; Bento et al. 2010), formed hydrogen-bonding networks with His ligands of the copper centers to maintain the geometry of the copper centers.

The reduction of the dioxygen and/or the release of the reduced water coordinated by two Asp residues at the TNC

Previous extensive studies have revealed that the reduction of O_2 to $2H_2O$ occurred at the TNC and involved two two-electron transfers (Augustine et al. 2010). The dioxygen was converted to the peroxide intermediate (PI) by first two-electron transfer, and this step was rate-limiting, followed by fast second two-electron reduction from PI to the native intermediate (NI) (Lee et al. 2002; Palmer et al. 2002; Yoon and Solomon 2007). In the decay of the PI to the NI, one proton was required to cleave the peroxide $^{-}$O–O^{-} bond (Palmer et al. 2002) and shuttled by a Glu residue nearby the TNC center (Chen et al. 2010; Bento et al. 2010). On the other hand, an Asp residue at the TNC, such as Asp116 in the CotA-laccase, Asp112 in the CueO-laccase, Asp106 in lacHB27, and Asp94 in Fet3p-metallo oxidase, was also important for the reduction of dioxygen to water (Silva et al. 2012; Hugo et al. 2015; Quintanar et al. 2005; Kataoka et al. 2009). This residue did not provide the proton but coordinated an OH^{-} ion and an H_2O molecule connecting the T2 Cu atom (Silva et al. 2012; Augustine et al. 2007; Bento et al. 2010).

In lacTT, the Asp106 residue was at the T3α-T2 edge, its carboxylate group, within the H-bond distances with the His402 ligand of the T3α Cu atom (3.85 Å) and the His95 ligand of the T2 Cu atom (2.71 Å), points towards the water-leaving channel (Figs. 3 and 8a). The bioinformatics studies demonstrate that this residue is equivalent to the Asp residue in other MCOs (Fig. S5) (Silva et al. 2012; Hugo et al. 2015; Quintanar et al. 2005; Kataoka et al. 2009). To get insight into the roles of the Asp106 residue, we mutated the Asp106 to leucine, arginine, and glutamic acid. The kinetic assay revealed that three mutants exhibited similar catalytic efficiency, ~4-fold decrease as compared with that of the wild-type laccase (Tables 1 and S3). CD spectra of the wild-type enzyme and three mutants show no significant difference (Fig. 4c), reflecting the similarity of their global structures. This was indicated by the structural superimposition of mutants with WT enzyme (Fig. S6B). However, there are some small differences at the Cu centers and in the orientations of the Cu ligands; Table S2 shows that in three mutants, the distance between each two Cu atoms at the TNC becomes remarkably longer as compared with that of the wild-type enzyme. Furthermore, in the D106E mutant, one carboxyl O atom of the side chain of E106 still points to the water-leaving channel, but the other orientates to the interior of the protein (Fig. 8b). Although the substitution of the D106 residue by glutamic acid retained the positive charge at this position, the increase of side chain length caused the change of interacting networks at the TNC, and the increases of the COO^{-}_{E106}-N^{δ}_{H95} distance from 2.71 to 4.26 Å (Fig. 8b) and the COO^{-}_{E106}-N^{δ}_{H402} distance from 3.85 to 4.06 Å. These changes may contribute to

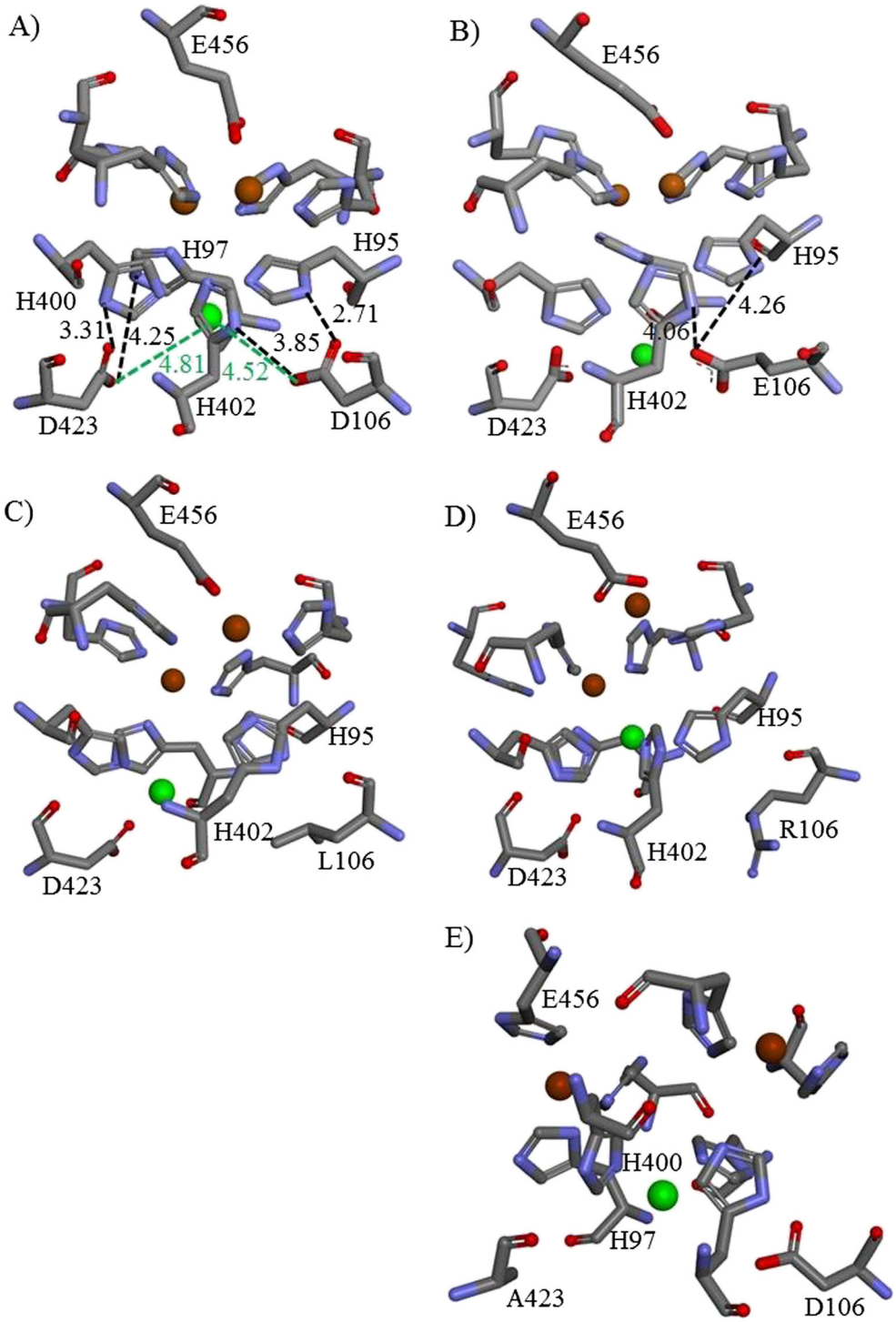

Fig. 8 Hydrogen-bonding networks formed between the amino acid residue at the position of 106/423 and the histidine ligands of the copper centers. **a** In the wild-type lacTT. **b** In the D106E mutant. **c** In the D106L mutant. **d** In the D106R mutant. **e** In the D423A mutant

the decrease in the catalytic efficiency of the D106E mutant. In D106L mutant, the side chain of the apolar leucine residue points to the water-leaving channel and His ligands of the Cu center, but there are no H-bond interactions between them (Fig. 8c). In the case of the D106R mutant, negatively charged side chain of the arginine residue oriented to the opposite direction of the Asp residue in WT enzyme. The histidine ligands of the T3α and T2 Cu atoms cannot form H-bond interactions with the R106 residue any more (Fig. 8d). These findings suggest that the D106 residue is involved in the catalytic reaction by hydrogen-bonding networks to the histidine ligands of the Cu centers.

In UV-visible spectra, compared with the WT enzyme, the D106E, D106R, and D106L mutants show lower intensity peak at 330 nm, suggesting the Cu occupancy of the Cu sites at the TNC is lower, consistent with the loose structure of the

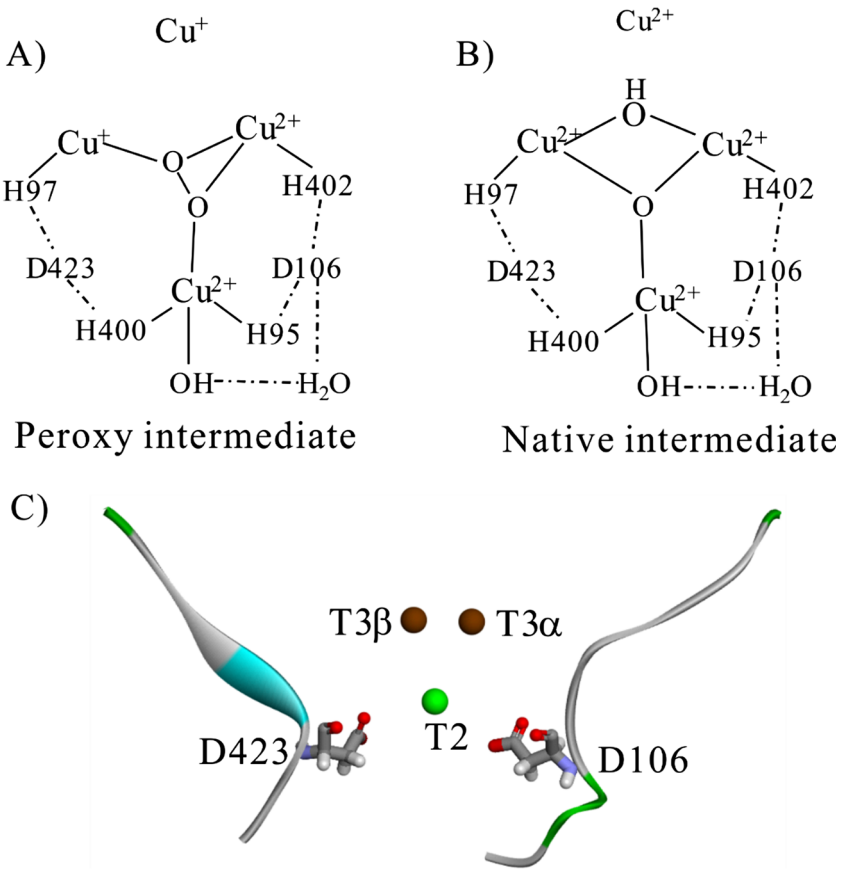

Fig. 9 The schematic diagram of two intermediates, peroxide intermediate (**a**) and native intermediate (**b**), in the catalytic cycle of the laccase. In two intermediates, the D423 residue formed the hydrogen-bonding interactions with H97 of T3β Cu and H400 of T2 Cu; the D106 residue H-bound with H402 of T3α Cu and H95 of T2 Cu, and formed a network with a water and a hydroxyl connecting with the T2 Cu atom. **c** Two acidic residues at the TNC were symmetrically distributed at both sides of the T2 Cu atom, and their side chains pointed towards the water-leaving channel. The D423 residue was at a β-sheet and at the inner of the channel, while the D106 residue was located at the exit of the channel, and at a flexible loop

TNC demonstrated by the longer distance between two Cu atoms in mutants (Table S2). For the peak at 608 nm, the higher intensity was observed for the D106E and D106L mutants, while the D106R enzyme shows a lower intensity peak, reflecting different occupancy at the T1 Cu site in three mutants.

The Asp423 and Asp106 residues are symmetrically distributed at both sides of the T2 Cu atom (Fig. 8a). The D423 residue is situated at the T2-T3β side and at the water-leaving channel. The carboxyl side chain of the D423 residue also points towards the water-leaving channel (Fig. 3), within hydrogen-bonding distances with the His97 ligand of T3β Cu and the His400 ligand of T2 Cu. Thus, both Asp residues may play the key roles in the catalytic activity of lacTT. To address the importance of the D423 residue in interacting networks with His ligands, the D423 residue was replaced by an apolar alanine. In this case, the catalytic efficiency of the D423A mutant was 46% of the WT enzyme. Considering that the Cu loading at the T1 Cu site in the D423A mutant was 70% of the WT enzyme, reflected by the lower intensity of the peak at 608 nm in the UV-visible spectrum of the D423A mutant (Fig. 2d and Table S3), thus, the catalytic efficiency of the D423A mutant was adjusted to ~65% of the WT enzyme. Again, the A423 residue could not form H-bond interactions with His400 bound to the T2 Cu atom and His97 bound to the T3β Cu atom (Fig. 8a, e). In the D423A mutant, the alteration in the orientation of the His ligands may damage the catalytic behavior of the enzyme. It is interesting that the lack of the interactions in the D423A mutant did not lead to the alterations of the distance between the Cu atoms at the TNC (Table S2) and the overall structure of the enzyme (Figs. 4d and S6D).

Discussion

Laccase within the multicopper oxidase family appears to share similar structural characteristics, including absolutely conserved histidine ligands of the active Cu centers which form the primary copper coordination sphere (Hugo et al. 2015; Quintanar et al. 2005; Augustine et al. 2007; Kataoka et al. 2009; Ueki et al. 2006). The N-terminal amino group of histidine ligates the Cu. Its orientation and/or position is directly related to the catalytic activity of the enzyme. Noncovalent secondary sphere residues around the primary coordinating ligands affect the catalysis of the enzyme by steric, electrostatic, and/or hydrogen-bonding interactions. Hydrogen-bonding network formed by secondary sphere residues was found to be most common in O_2-activating enzymes (Chen et al. 2010; Span et al. 2017). They play an important

role in stabilizing coordination geometries, adjusting ligand donor strengths, and mediating proton transfer reactions (Span et al. 2017; Holm et al. 1996; Makris et al. 2007).

In this study, the structure of lacTT was predicted by using homology modeling. It exhibits an overall folding similar to that of other multiple copper oxidases, comprising of three domains and four copper atoms. Four second-sphere residues, E356, E456, D106, and D423, were identified, and their roles were analyzed and discussed. It was suggested that the E356 residue maintains the geometry of the T1 Cu site by interacting with His ligands and may be related to the binding of the substrate revealed by site-directed mutagenesis of the E356 residue.

The E456 residue was situated at the entry channel of dioxygen. It is highly conserved in MCOs. The substitution of the E456 residue by aspartic acid, arginine, or leucine was used to examine its role. The replacement of this residue did not lead to change of the overall structures (Figs. 4 and S6C). But the E456D mutant shows a fivefold lower efficiency of the wild-type enzyme (Table 1), consistent with the ability of the Asp residue to shuttle the proton. The efficiency of the E456D mutant decreased due to the alteration of interacting networks at the Cu centers (Fig. 7). Similar behavior was observed for the CotA laccase (Chen et al. 2010). However, the difference in the catalytic behavior was also found between CotA and lacTT enzymes. For the CotA laccase, equivalent Glu498 residue was mutated to leucine or threonine, no enzymatic activity was noted (Chen et al. 2010). In contrast, for lacTT, the E456R and E456L mutants could not have the ability to shuttle the proton, but they still showed 3 and 4% activity of the wild-type enzyme, respectively. One explanation is that there was an alternative proton transfer pathway in lacTT although the transfer efficiency was very low. Or the solvent entered the TNC, acting as a proton donor, retrieved the activity to some extent. On the other hand, structural data of lacTT indicate that there are hydrogen-bonding networks established between the E456 residue and His ligands of the T3α and T3β Cu atoms (Fig. 7a). The replacement of this residue leads to a loose structure at the TNC, increasing the distance between the Cu atoms (Table S2), which can decrease the electron transfer rate in the protein. It is suggested that the E456 residue can be required to maintain the geometry of TNC. Two functions of the E456 residue may be explained by two conformations—one conformation is the protonated state, which can provide the proton to the peroxide bond, and the other one is the carboxylate state, which can maintain the geometry of the TNC by forming hydrogen-bonding networks with His ligands of the cupper ions. At the optimal reaction condition of pH 6.0, the Glu456 residue can be present in the carboxylate state considering the pK_a value of 3.4 in solution, while it can also be abnormally protonated as described in CotA laccase depending on the oxidation and TNC loading state (Bento et al. 2010). Two states of the Glu456 residue may be actualized by conformational dynamics. X-ray crystallographic studies show that equivalent Glu451 residue in lacHB27 is present in both conformations (Hugo et al. 2015).

In the catalytic cycle of MCOs, two intermediates (PI and NI) were established experimentally. In the peroxy intermediate, three copper ions at the TNC coordinate the O-O bond, while the T2 Cu ion had a coordinating hydroxide (Yoon and Solomon 2007) (Fig. 9a). In the native intermediate, the O-O bond was cleaved and the oxygen atoms presented as a μ3-oxo with three copper atoms at the TNC and a μ2-OH bridging two T3 Cu ions (Yoon et al. 2007) (Fig. 9b). In both intermediates, the D106 and D423 residues in lacTT could H-bond to His ligands of T2 Cu and T3 Cu (Fig. 9a, b). These hydrogen-bonding networks can increase the nucleophilicity of the N-terminal amino group of histidine ligands and facilitate the stability of oxyl intermediates at the TNC (Fig. 9a, b) (Span et al. 2017; Yoon and Solomon 2007; Yoon et al. 2007). It is worth noticing that when the D106 and D423 residues are mutated to an apolar residue, the activities of two mutants display significant differences. The catalytic efficiency of the D106L mutant was 2.5-fold lower than that of the D423A mutant (Tables 1 and S3) considering the Cu loading at the T1 Cu site in two mutants (Fig. 2c, d). This can be explained by another role of the D106 residue. The D106 residue may mediate the release of the reduced water. Structural data show that the D423 residue is located at the inner of the water-leaving channel at the β-sheet in domain 1. The D106 residue is situated at the exit of the water-leaving channel at the solvent-exposed loop in domain 3 (Figs. 3 and 9c). The flexibility of this loop can provide for the opportunity of the D106 residue switching between two functions. The mutation of the D106 residue to leucine did not only damage the hydrogen-bonding networks but also lost the ability to carry the water. This role of the D106 residue was also observed in other MCOs (Hugo et al. 2015; Quintanar et al. 2005; Augustine et al. 2007; Kataoka et al. 2009; Ueki et al. 2006). X-ray studies indicate that the Asp106 residue in lacHB27 does not take part in both the provision of the proton and the cleavage of the O-O bond, but coordinated a water molecule and a hydroxyl group (Hugo et al. 2015).

In summary, two acidic residues, Glu456 and Asp106 in lacTT, were examined, and they exhibit a role similar to that of equivalent acidic residues in other MCOs as described in previous work (Hugo et al. 2015; Quintanar et al. 2005; Augustine et al. 2007; Kataoka et al. 2009; Ueki et al. 2006). In addition, we, for the first time, identified two key second-sphere residues, E356 and Asp423, and discussed their roles. Four second-sphere residues affect the activity of the enzyme, mainly via hydrogen-bonding networks.

Funding This study was supported by the National Natural Science Foundation of China (No. 41673074) and the Science and Technology

Planning Project of Guangzhou City (No. 201607010073) to X Yang. All the authors are thankful for the financial support of the Science and Technology Planning Project of Guangzhou City (No. 201607010307).

Compliance with ethical standards

This article does not contain any studies with human participants or animals by any of the authors.

Conflict of interest The authors declare that they have no competing interests.

References

Augustine AJ, Quintanar L, Stoj CS, Kosman DJ, Solomon EI (2007) Spectroscopic and kinetic studies of perturbed trinuclear copper clusters: the role of protons in reductive cleavage of the O-O bond in the multicopper oxidase Fet3p. J Am Chem Soc 129:13118–13126. https://doi.org/10.1021/ja073905m

Augustine AJ, Kjaergaard C, Qayyum M, Ziegler L, Kosman DJ, Hodgson KO, Hedman B, Solomon EI (2010) Systematic perturbation of the trinuclear copper cluster in the multicopper oxidases: the role of active site asymmetry in its reduction of O_2 to H_2O. J Am Chem Soc 132:6057–6067. https://doi.org/10.1021/ja909143d

Bello M, Valderrama B, Serranoposada H, Rudiñopiñera E (2012) Molecular dynamics of a thermostable multicopper oxidase from *Thermus thermophilus* HB27: structural differences between the apo and holo forms. PLoS One 7:e40700. https://doi.org/10.1371/journal.pone.0040700

Bento I, Silva CS, Chen Z, Martins LO, Lindley PF, Soares CM (2010) Mechanisms underlying dioxygen reduction in laccases. Structral and modelling studies focusing on proton transfer. BMC Struct Biol 10:28–42. https://doi.org/10.1186/1472-6807-10-28

Chen Z, Durão P, Silva CS, Pereira MM, Todorovic S, Hildebrandt P, Bento I, Lindley PF, Martins LO (2010) The role of Glu498 in the dioxygen reactivity of CotA-laccase from *Bacillus subtilis*. Dalton Trans 39:2875–2882. https://doi.org/10.1039/b922734b

Cole JL, Clark PA, Solomon EI (1990) Spectroscopic and chemical stuides of the laccase trinuclear copper active site: geometric and electronic structure. J Am Chem Soc 112:9534–9548

Durao P, Bento I, Fernandes AT, Melo EP, Lindley PF, Martins LO (2006) Perturbations of the T1 copper site in the CotA laccase from *Bacillus subtilis*: structural, biochemical, enzymatic and stability studies. J Biol Inorg Chem 11:514–526. https://doi.org/10.1007/s00775-006-0102-0

Dwivedi UN, Singh P, Pandey VP, Kumar A (2011) Structure and function relationship among bacterial, fungal and plant laccases. J Mol Catal B-Enzym 68:117–128. https://doi.org/10.1016/j.molcatb.2010.11.002

Enguita FJ, Martins LO, Henriques AO, Carrondo MA (2003) Crystal structure of a bacterial endospore coat component. A laccase with enhanced thermostability properties. J Biol Chem 278:19416–19425. https://doi.org/10.1074/jbc.M301251200

Enguita FJ, Marçal D, Martins LO, Grenha R, Henriques AO, Lindley PF, Carrondo MA (2004) Substrate and dioxygen binding to the endospore coat laccase from *Bacillus subtilis*. J Biol Chem 279:23472–23476. https://doi.org/10.1074/jbc.M314000200

Giardina P, Faraco V, Pezzella C, Piscitelli A, Vanhulle S, Sannia G (2010) Laccases: a never-ending story. Cell Mol Life Sci 67:369–385. https://doi.org/10.1007/s00018-009-0169-1

Holm RH, Kennepohl P, Solomon EI (1996) Structural and functional aspects of metal sites in biology. Chem Rev 96:2239–2314. https://doi.org/10.1007/s00018-009-0169-1

Hugo SP, Sara CL, Sonia Patricia RT, Claudia RA, Vivian S, Enrique ROPE (2015) X-ray-induced catalytic active-site reduction of a multicopper oxidase: structural insights into the proton-relay mechanism and O2-reduction states. Acta Crystallogr D Biol Crystallogr 71:2396–2411. https://doi.org/10.1107/S1399004715018714

Jones SM, Solomon EI (2015) Electron transfer and reaction mechanism of laccases. Cell Mol Life Sci 72:869–883. https://doi.org/10.1007/s00018-014-1826-6

Kallio JP, Auer S, Jänis J, Andberg M, Kruus K, Rouvinen J, Koivula A, Hakulinen N (2009) Structure-function studies of a *Melanocarpus albomyces* laccase suggest a pathway for oxidation of phenolic compounds. J Mol Biol 392:895–909. https://doi.org/10.1016/j.jmb.2009.06.053

Kataoka K, Komori H, Ueki Y, Konno Y, Kamitaka Y, Kurose S, Tsujimura S, Higuchi Y, Kano K, Seo D (2007) Structure and function of the engineered multicopper oxidase CueO from *Escherichia coli*—deletion of the methionine-rich helical region covering the substrate-binding site. J Mol Biol 373:141–152. https://doi.org/10.1016/j.jmb.2007.07.041

Kataoka K, Sugiyama R, Hirota S, Inoue M, Urata K, Minagawa Y, Seo D, Sakurai T (2009) Four-electron reduction of dioxygen by a multicopper oxidase, CueO, and roles of Asp112 and Glu506 located adjacent to the trinuclear copper center. J Biol Chem 284:14405–14413. https://doi.org/10.1074/jbc.M808468200

Lee SK, George SD, Antholine WE, Hedman B, Hodgson KO, Solomon EI (2002) Nature of the intermediate formed in the reduction of O_2 to H_2O at the trinuclear copper cluster active site in native laccase. J Am Chem Soc 124a:6180–6193

Liu H, Cheng Y, Du B, Tong C, Liang S, Han S, Zheng S, Lin Y (2015) Overexpression of a novel thermostable and chloride-tolerant laccase from *Thermus thermophilus* SG0.5JP17-16 in *Pichia pastoris* and its application in synthetic dye decolorization. PLoS One 10:e0119833. https://doi.org/10.1371/journal.pone.0119833

Makris TM, von Koenig K, Schlichting I, Sligar SG (2007) Alteration of P450 distal pocket solvent leads to impaired proton delivery and changes in heme geometry. Biochemistry 46:14129–14140. https://doi.org/10.1021/bi7013695

Malmstrom BG (1982) Enzymology of oxygen. Annu Rev Biochem 51:21–59. https://doi.org/10.1146/annurev.bi.51.070182.000321

Marcus RA, Sutin N (1985) Electron transfers in chemistry and biology. Biochim Biophys Acta 811:265–322

Matera I, Gullotto A, Tilli S, Ferraroni M, Scozzafava A, Briganti F (2008) Crystal structure of the blue multicopper oxidase from the white-rot fungus *Trametes trogii* complexed with p -toluate. Inorg Chim Acta 361:4129–4137

Nakamura K, Go N (2005) Function and molecular evolution of multicopper blue proteins. Cell Mol Life Sci 62:2050–2066. https://doi.org/10.1007/s00018-004-5076-5

Palmer AE, Quintanar L, Severance S, Wang T, Kosman DJ, Solomon EI (2002) Spectroscopic characterization and O2 reactivity of the trinuclear Cu cluster of mutants of the multicopper oxidase Fet3p. Biochemistry 41:6438–6448

Pezzella C, Guarino L, Piscitelli A (2015) How to enjoy laccases. Cell Mol Life Sci 72:923–940. https://doi.org/10.1007/s00018-014-1823-9

Piontek K, Antorini M, Choinowski T (2002) Crystal structure of a laccase from the fungus *Trametes versicolor* at 1.90-A resolution containing a full complement of coppers. J Biol Chem 277:37663–37669. https://doi.org/10.1074/jbc.M204571200

Polyakov KM, Fedorova TV, Stepanova EV, Cherkashin EA, Kurzeev SA, Strokopytov BV, Lamzin VS, Koroleva OV (2009) Structure of native laccase from *Trametes hirsuta* at 1.8 Å resolution. Acta Crystallogr D Biol Crystallogr 65:611–617. https://doi.org/10.1107/S0907444909011950

Quintanar L, Stoj C, Wang T, Kosman DJ, Solomon EI (2005) Role of aspartate 94 in the decay of the peroxide intermediate in the

multicopper oxidase Fet3p. Biochemistry 44:6081–6091. https://doi.org/10.1021/bi047379c

Santhanam N, Vivanco JM, Decker SR, Reardon KF (2011) Expression of industrially relevant laccases: prokaryotic style. Trends Biotechnol 29:480–489. https://doi.org/10.1016/j.tibtech.2011.04.005

Silva CS, Damas JM, Chen Z, Brissos V, Martins LO, Soares CM, Lindley PF, Bento I (2012) The role of Asp116 in the reductive cleavage of dioxygen to water in CotA laccase: assistance during the proton-transfer mechanism. Acta Crystallogr D Biol Crystallogr 68:186–193. https://doi.org/10.1107/S0907444911054503

Solomon EI, Heppner DE, Johnston EM, Ginsbach JW, Cirera J, Qayyum M, Kieberemmons MT, Kjaergaard CH, Hadt RG, Li T (2014) Copper active sites in biology. Chem Rev 114:3659–3853. https://doi.org/10.1021/cr400327t

Solomon EI (2006) Spectroscopic methods in bioinorganic chemistry: blue to green to red copper sites. Inorg Chem 45:8012–8025. https://doi.org/10.1021/ic060450d

Span EA, Suess DLM, Deller MC, Britt RD, Marletta MA (2017) The role of the secondary coordination sphere in a fungal polysaccharide monooxygenase. ACS Chem Biol 12:1095–1103. https://doi.org/10.1021/acschembio.7b00016

Ueki Y, Inoue M, Kurose S, Kataoka K, Sakurai T (2006) Mutations at Asp112 adjacent to the trinuclear Cu center in CueO as the proton donor in the four-electron reduction of dioxygen. FEBS Lett 580:4069–4072. https://doi.org/10.1016/j.febslet.2006.06.049

Wherland S, Farver O, Pecht I (2014) Multicopper oxidases: intramolecular electron transfer and O 2 reduction. J Biol Inorg Chem 19:541–554. https://doi.org/10.1007/s00775-013-1080-7

Yoon J, Solomon EI (2007) J Am Chem Soc 129:13127–13136. Electronic structure of the peroxy intermediate and its correlation to the native intermediate in the multicopper oxidases: insights into the reductive cleavage of the O-O bond. https://doi.org/10.1021/ja073947a

Yoon J, Liboiron BD, Sarangi R, Hodgson KO, Hedman B, Solomon EI (2007) The two oxidized forms of the trinuclear cu cluster in the multicopper oxidases and mechanism for the decay of the native intermediate. Proc Natl Acad Sci U S A 104:13609–13614. https://doi.org/10.1073/pnas.0705137104